

Comparison of the Thermoresponsive Deswelling Kinetics of Poly(2-(2-methoxyethoxy)ethyl methacrylate) Hydrogels Prepared by ATRP and FRP

Jeong Ae Yoon, Chakicherla Gayathri, Roberto R. Gil, Tomasz Kowalewski,* and Krzysztof Matyjaszewski*

Department of Chemistry, Carnegie Mellon University, 4400 Fifth Avenue, Pittsburgh, Pennsylvania 15213

Received March 4, 2010; Revised Manuscript Received April 5, 2010

ABSTRACT: Thermoresponsive hydrogels based on 2-(2-methoxyethoxy)ethyl methacrylate (MEO₂MA) were prepared by both atom transfer radical polymerization (ATRP) and conventional free radical polymerization (FRP). The lower critical solution temperature (LCST) transitions of the hydrogels prepared by the different polymerization mechanisms were compared at the macroscopic level and the molecular level. Gels prepared by ATRP swelled much more, but their macroscopic deswelling was retarded in comparison with gels prepared by FRP. This retardation was especially pronounced at higher temperatures and was attributed to the enhanced formation of skin layer in uniform gels prepared by ATRP. Variable-temperature time-lapse NMR spectroscopy showed that the rate of the dehydration of polymer chains at molecular level was much faster than macroscopic deswelling.

Introduction

Stimuli-responsive polymers^{1–4} change their physical properties in response to external triggers such as temperature, pH, light, or other applied external fields. Stimuli-responsive hydrogels, water-swallowable cross-linked stimuli-responsive polymers, have been extensively studied due to their potential applications such as drug delivery systems,^{5–7} responsive membranes,^{8–10} molecular machines,^{11–14} and nanotemplates for nanoparticles.^{15–17} Typically, hydrogels for these applications rely on a thermoresponsive volume phase transition at a lower critical solution temperature (LCST). The most often studied LCST system is based on poly(*N*-isopropylacrylamide) (pNIPAAm).^{18–20} Other successful thermoresponsive systems, with an LCST tunable between 20 and 80 °C, include oligo(ethylene glycol) methacrylates with a few ethylene oxide repeating units.^{21–26} Since they are based on derivatives of biocompatible poly(ethylene oxide) (PEO), they are generally nontoxic and thus are promising candidates for bio-related applications.

Recently, controlled radical polymerization techniques (CRP)^{27–30} have been actively applied to the preparation of hydrogels. The procedures include not only preparation of the gel matrix by CRP but also further modification of gels prepared by either conventional free radical polymerization (FRP) or CRP.^{31–34} CRP procedures have also played an important role by facilitating the preparation of specific building units of gellators, such as triblock copolymers, hyperbranched polymers, or nanogels.^{35–39} Gellators form three dimensionally cross-linked macrogels through physical cross-linking such as hydrophobic aggregations or ionic interactions.

Hydrogels prepared by CRP (CRP gels) possess several advantages over gels prepared by FRP (FRP gels). For example, CRP gels exhibit higher swelling ratios due to the more homogeneous network structure.^{40–43} Fast initiation, slow propagation, and minimized termination reactions provide sufficient time

for the primary chains to relax during each activation cycle. Therefore, the propagating radical chain ends have a greater chance to react with pendant vinyl groups present on other primary chains, forming branching points. Conversely, radical ends of growing FRP chains have greater chance to react with their own pendant vinyl groups to form a densely cross-linked nanogel, which is barely swellable. Another advantage of CRP gels comes from the fact that the gelation occurs via linkage of preformed hyperbranched polymers. The branched chain ends remain in the network as dangling chains and accelerate the rate of a transition owing to their greater conformational freedom.³⁴ Moreover, the primary polymer chain ends in CRP preserve functional groups that can be further used for incorporation of other chemical species.^{44,45} CRP gels are also preferred when a degradable material is desired, owing to the predeterminable molecular weight and narrow molecular weight distribution of decomposed fragments, and reduce the possibility of residues with a molecular weight above the renal threshold.^{46–52}

Herein, atom transfer radical polymerization (ATRP),^{53–57} one of the most successful CRP techniques, was used to prepare hydrogels based on 2-(2-methoxyethoxy)ethyl methacrylate (MEO₂MA). The gel deswelling process was systematically studied, not only macroscopically but also at the molecular level. At the macroscopic level, automated analysis of time-lapse images of gels undergoing thermal transition was performed in addition to the conventional gravimetry. Variable-temperature time-lapse NMR spectroscopy was performed to provide molecular level insights into the LCST transition. Although the synthesis of MEO₂MA hydrogels by ATRP and the thermoresponsive LCST transitions have been demonstrated and evaluated in the past, a systematic comparison of the effect of polymerization method on deswelling kinetics had not yet been conducted, and thus it became the main focus of the present work.

Experimental Section

Synthesis of an ATRP Gel. MEO₂MA (3.00 mL, 16.8 mmol), 2-hydroxyethyl methacrylate (HEMA, 39 μL, 0.32 mmol),

*Corresponding authors. E-mail: tomek@andrew.cmu.edu (T.K.), km3b@andrew.cmu.edu (K.M.).

ethylene glycol dimethacrylate (EGDMA, 31 μ L, 0.17 mmol), ethyl 2-bromoisobutyrate (EBiB, 5.0 μ L, 0.032 mmol), *N,N,N',N'',N'''*-pentamethyldiethylenetriamine (PMDETA, 7.0 μ L, 0.032 mmol), and anisole (0.5 mL) were added to a 10 mL Schlenk flask. The molar ratio of MEO₂MA:HEMA:EGDMA:EBiB:PMDETA:CuBr was 500:10:5:1:1:1. Pieces of glass tubing (i.d.: 3 mm; length: around 1.5 cm) were placed into the flask as cylindrical shape templates. The pregel reaction mixture was degassed by subjecting the flask to three freeze–pump–thaw cycles. Next, CuBr (4.6 mg, 0.032 mmol) was added to the flask under nitrogen flow. A small amount of the reaction mixture (ca. 0.02 mL) was taken by syringe and diluted with acetone. The acetone solution was analyzed by gas chromatography (GC) to calculate the initial peak intensity of MEO₂MA compared to that of anisole, the internal standard. The flask was placed in an oil bath preheated to the selected reaction temperature (60 or 70 °C). The stirring was stopped when the solution became viscous in order to minimize the amount of bubbles trapped inside the gel. After a predetermined reaction time, 2 h at 70 °C or 5 h at 60 °C, the reaction was stopped by opening the flask and exposing the contents to air. A small piece of gel (ca. 0.05 g) was taken and immersed in acetone (ca. 1 mL) overnight. The acetone solution was used for the GC analysis to calculate the final peak intensity of unreacted MEO₂MA remaining in the gel mixture. The MEO₂MA conversion was calculated based on the GC results taken before and after gelation. The method of gel purification is described in the Supporting Information.

Synthesis of a FRP Gel. MEO₂MA (3 mL, 16.8 mmol), HEMA (39 μ L, 0.32 mmol), EGDMA (31 μ L, 0.17 mmol), and anisole (0.5 mL) were added to a 10 mL Schlenk flask. Pieces of glass tubing (i.d.: 3 mm; length: around 1.5 cm) were added as gel templates and the solution was degassed by three freeze–pump–thaw cycles. Then, AIBN (5.3 mg, 0.032 mmol) was added to the flask under nitrogen flow. The rest of the gelation and the purification procedures were same as in the ATRP method.

Kinetic Studies of Relative Volume Change upon Deswelling Using a Gravimetric Method. The fundamentals of this method are explained in many reports.^{19,34,58,59} The deswelling kinetics is often expressed in terms of water retention (eq 1), which characterizes the ability of a hydrogel to expel water upon change of conditions (e.g., increase of temperature above LCST), and is defined as the weight of water retained inside a hydrogel versus the weight of initially absorbed water. *Water retention* can be contrasted with the *swelling ratio*, which, in turn, characterizes the total “water capacity” of the hydrogel and, according to eq 2, is defined as the ratio of weight of water contained within the swollen hydrogel to its dry weight. In this paper, volume has comparable meaning to weight if one assumes that the gel density is close to 1 g/cm³.

$$\text{water retention } (t) = \frac{w_t - w_d}{w_0 - w_d} \quad (1)$$

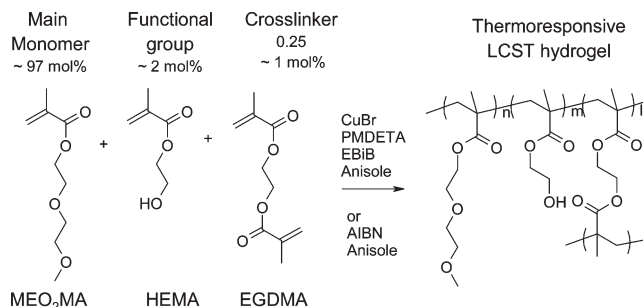
$$\text{swelling ratio } (t) = \frac{w_t - w_d}{w_d} \quad (2)$$

where w_t , w_d , and w_0 are weights of deswelling hydrogel at time t , of dried gel, and of hydrogel at an equilibrium below the LCST.

Quasi-Volumetric Investigation of Gel Deswelling by Image Analysis. A fully swollen piece of hydrogel kept initially under water at 4 °C was transferred directly into water bath maintained at the experiment temperature (30–60 °C), and digital images were taken every 8 s for 30–60 min. The images were analyzed by a custom code written in MATLAB 7.0 (Mathworks, Natick, MA) to calculate the relative volume decrease over time. The detailed description is provided in the Supporting Information.

¹H NMR Studies of the Hydration and Dehydration. Dried cylindrical samples of gels with a typical diameter of 3 mm and

Scheme 1. Synthesis of a Thermoresponsive LCST Hydrogel Based on MEO₂MA



average length of 10 mm were placed in 5 mm NMR tubes. The tubes were filled with D₂O and refrigerated at 4 °C for more than 1 week to allow the dried gels to fully expand in the NMR tubes. For studies of the dehydration dynamics, the gel samples were transferred from the refrigerator into the NMR probe held above the LCST, and the spectra were acquired as a function of time immediately after insertion and locking. The time evolution of the NMR spectra was evaluated by following a normalized intensity ($t = 2$ s) of the 3.2 ppm methoxy peak in the spectra deconvoluted into four Lorentzians (for details, see the Supporting Information).

Results and Discussion

1. Synthesis. Hydrogels with different amount of cross-linker were prepared under different reaction conditions using different mechanisms, ATRP and FRP (Scheme 1). The hydrogels were named according to the following rules: the first letter A or F represents the mechanism, ATRP or FRP, respectively; the second letter H or L represents the high or low cross-link density; the final number 1 or 2 represents the reaction conditions: a reaction temperature of 70 °C and a reaction time of 120 min, or a reaction temperature of 60 °C and a reaction time of 300 min, respectively. Thus, for example, gel AH1 was prepared by using ATRP mechanism, contained high cross-link density, and the reaction was done at 70 °C for 120 min. The structures of gels are summarized in Table 1.

Ratio 1:100 of EGDMA:MEO₂MA was used for samples AH1, AH2, FH1, and FH2 (H gels) with *high* cross-linker content, while ratio 1:400 was used for samples AL1, AL2, and FL2 (L gels) with *low* cross-linker content. The smaller amount of initiator was used for L gels, in order to satisfy a gel formation condition, $[\text{EGDMA}]/[\text{initiator}] > 1$.^{60,61} A mole ratio of HEMA to MEO₂MA of 2:100 was also used for a potential modification of the gel structure.⁶² The gel composition was calculated based on the conversion of MEO₂MA and an assumption of similar reactivity for all vinyl groups in the reaction medium. Under conditions of the reaction temperature of 70 °C and the reaction time of 120 min, the gel conversion was less predictable, presumably due to the limited flowability of the solution. The faster increase in viscosity at a higher temperature should further limit the movements of primary chains and monomers and yield a gel at lower conversion. Therefore, the hydrogels prepared under conditions of the reaction temperature of 60 °C and the reaction time of 300 min were more suitable for comparison of kinetics due to the comparable conversions ($\geq 95\%$).

Gravimetrically measured swelling ratios at equilibrium below LCST (4 °C) are shown in Table 1. Clearly, swelling ratios of ATRP gels are higher than the swelling ratios measured for FRP gels with similar compositions. This can

Table 1. Preparation of Hydrogels

entry	mechanism	soln composition gel composition	conditions	conversion ^f	swelling ratio ^g
AH1	ATRP	500:10:5:1 ^a (315:6.3:4.3:1) ^e	70 °C, 120 min	63	4.0
AH2	ATRP	500:10:5:1 ^a (475:9.5:5:1) ^e	60 °C, 300 min	95	3.1
FH1	FRP	500:10:5:1 ^b (500:10:5:1) ^e	70 °C, 120 min	> 99	2.1
FH2	FRP	500:10:5:1 ^b (500:10:5:1) ^e	60 °C, 300 min	99	2.2
AL1	ATRP	625:12.5:1.56:1 ^c (556:11.1:1.54:1) ^e	70 °C, 120 min	89	8.9
AL2	ATRP	625:12.5:1.56:1 ^c (593:11.9:1.56:1) ^e	60 °C, 300 min	95	5.5
FL2	FRP	625:12.5:1.56:1 ^d (619:12.4:1.56:1) ^e	60 °C, 300 min	99	3.2

^a[MEO₂MA]/[HEMA]/[EGDMA]/[EBiB]/[PMDETA]/[CuBr] = 500/10/5/1/1/1. ^b[MEO₂MA]/[HEMA]/[EGDMA]/[AIBN] = 500/10/5/1. ^c[MEO₂MA]/[HEMA]/[EGDMA]/[EBiB]/[PMDETA]/[CuBr] = 625:12.5:1.56:1:1:1. ^d[MEO₂MA]/[HEMA]/[EGDMA]/[AIBN] = 625:12.5:1.56:1. ^eGel compositions were calculated based on the conversion values of MEO₂MA measured by GC, with the assumptions of equal reactivities of all vinyl groups and quantitative initiation efficiencies. ^fConversion of MEO₂MA measured by GC. ^gSwelling ratio at equilibrium measured at 4 °C (error range < 5% in all measurements).

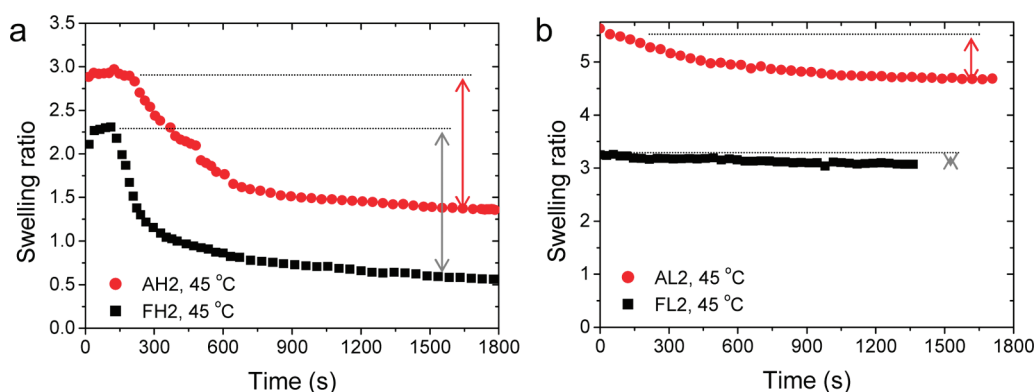


Figure 1. Comparison of swelling ratios upon deswelling of gels with high-cross-link density (a, gel AH2 and gel FH2) and gels with low-cross-link density (b, gel AL2 and gel FL2) at 45 °C.

be attributed to the reduced formation of collapsed nanogel domains in the gels prepared by a CRP procedure.^{40–42}

2. Macroscopic Deswelling Kinetics. Deswelling kinetics of hydrogels above LCST (> 22 °C) was observed by following the decrease of volume or weight over time. Those changes were converted to the decrease of water retention or swelling ratio, defined in eqs 1 and 2. The water retention and swelling ratio were determined by analyzing the snapshot images taken during the deswelling of the hydrogels and compared to the results from conventional gravimetry. As the two independently obtained results were in good agreement (Supporting Information, Figure SI2), only the results based on image analysis are reported in this paper.

The decrease of swelling ratios with time at 45 °C for gels prepared by ATRP and FRP at different cross-link densities is illustrated in Figure 1. The swelling ratio is defined as the weight of retained water per weight of dried gel. Therefore, the decrease in swelling ratio represents the absolute amount of water released. The gel AH2 swelled much more than gel FH2 but released a comparable amount of water (Figure 1a). This also indicates that a larger amount of water was retained in gel AH2. This can be due to the more pronounced “skin” effect, as will be discussed later. This skin effect depends, however, on cross-link density. Gel AL2 swelled more than gel FL2, and it also released more water on deswelling. Despite the larger initial swelling, the total amount of water released was smaller for gels with lower cross-link density due to more pronounced skin effect (Figure 1b).

In addition to evaluating the absolute amount of released water, the fraction of released water relative to initially absorbed water (water retention) was analyzed. The deswelling kinetics of highly cross-linked H gels at different temperatures are illustrated in Figure 2. The deswelling of the ATRP gel AH2 revealed a much longer retardation period at 45 and 60 °C than at 30 °C (see inset, Figure 2a). This retardation was attributed to the formation of a skin layer, followed by the skin rupture and release of water molecules through the generated cracks. Although faster deswelling was expected at the higher temperature (60 °C) for AH2, the deswelling was actually slower than at lower temperatures. This behavior can be explained by the formation of an even thicker skin layer at the very early stage at 60 °C, leading to the extended retardation period up to 100 s, further hindering water release. On the other hand, the LCST transition at a lower temperature (30 °C) was relatively slow; hence, the skin formation was diminished. In contrast, FRP gel FH2 deswelled at the slowest rate at 30 °C. The early retardation period at 45 or 60 °C was shorter for FH2 than AH2. Moreover, the deswelling after the retardation period was faster than in the case of AH2. This implies that the deswelling rate of FH2 was not strongly affected by the presence of a skin layer. The lower tendency of FRP gel to form a skin layer can be attributed to its greater heterogeneity and in particular to the presence of densely cross-linked nanogel domains. A densely cross-linked fraction of the gel has a higher LCST temperature than the other portions of the gel

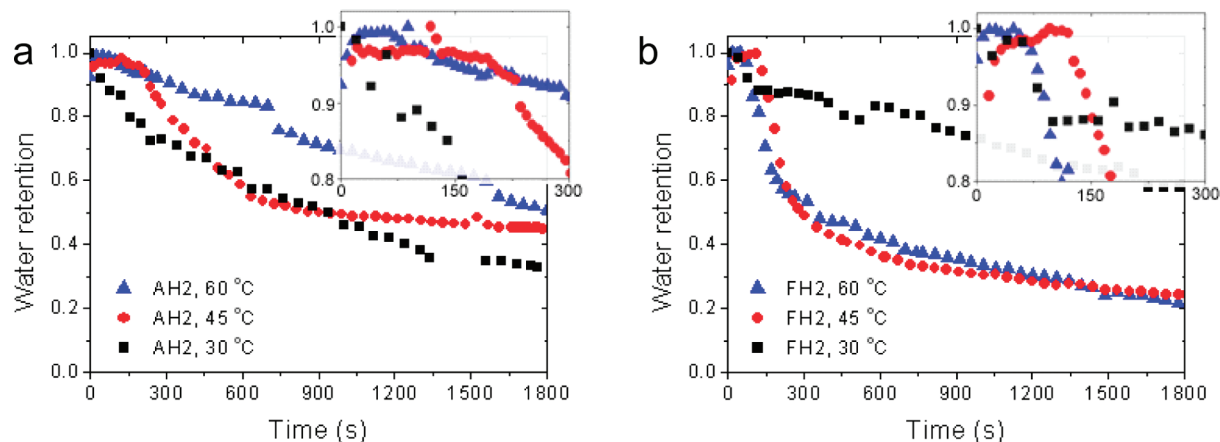


Figure 2. Comparison of water retention upon deswelling of high-cross-link density gels (H gels) prepared by ATRP (a, gel AH2) and FRP (b, gel FH2).

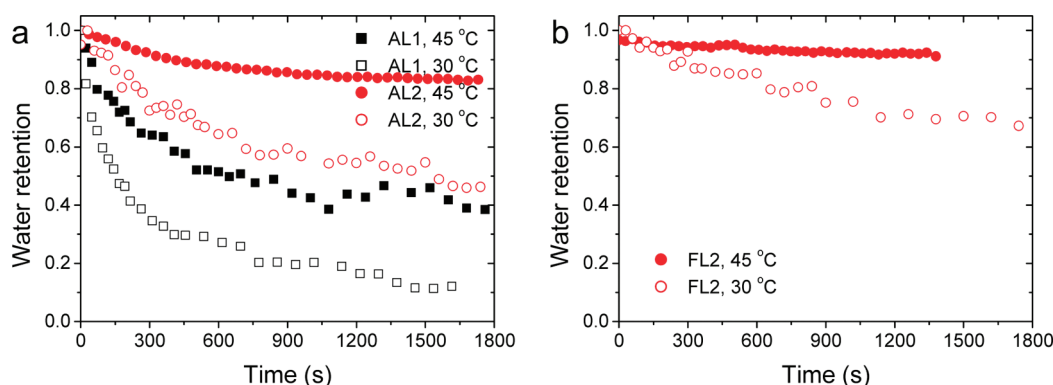


Figure 3. Comparison of water retention upon deswelling of low-cross-link density gels (L gels) prepared by ATRP (a, gel AL1 and AL2) and FRP (b, gel FL2).

and retains its hydrophilic nature during the LCST transition for a longer time. Although the dense domains limit the swelling ratio, they provide hydrophilic channels for water molecules to diffuse out. Previous studies^{63,64} have already pointed out that the presence of denser cross-linked domains is a way to introduce heterogeneity^{65–67} to a network structure. Under the absence of the significant skin effect, the deswelling rate of FH2 increased with the increase of temperature as a result of the increased magnitude of hydrophobic aggregation force. The slowest deswelling at 30 °C can be explained by the smallest magnitude of the hydrophobic aggregation force.

The deswelling kinetics of low-cross-link density gels (L gels) are presented in Figure 3. In all cases, the rate of deswelling was faster at the lower temperature (30 °C), indicating that a significant skin layer was formed at 45 °C. The deswelling of FL2 was very slow at 45 °C, suggesting that a certain degree of cross-linking (or cross-linker amount) is required for discussed heterogeneity to play a role in deswelling kinetics. The amount of cross-linker present in sample FH2 was apparently below this limit, and the sample was affected by the skin layer. The rate of deswelling of the samples at a given temperature was related to the equilibrium swelling ratio (Table 1). Higher swelling gels had lower cross-linking density and deswelled faster. This can be attributed to the more rapid transition of less cross-linked networks. The LCST transition rate is discussed further in the following section.

3. Dehydration Kinetics at Molecular Level. Variable-temperature time-lapse NMR spectroscopy was performed

to obtain the molecular level insights into dehydration kinetics of the hydrogels. ¹H NMR spectra of the gels were recorded at a given temperature as a function of time, and the progressive line broadening was used as a measure of the extent of dehydration. The spectra were then fitted to a sum of four Lorentzians plus a constant baseline, and the decrease of peak heights was used as a measure of their broadening (Figure 4). It should be noted that not all NMR spectra were suitable for this type of analysis. For example, the NMR spectra of AH2, FH1, and FH2 were too broad to attempt accurate deconvolution (cf. Supporting Information, Figure SI4). Since the initial NMR spectra were in general sharper for lower cross-link density L gels, the following discussion of molecular level dehydration kinetics is focused on these materials.

All further discussion is based on the time evolution of the peak at 3.2 ppm (–OCH₃ of MEO₂MA, Supporting Information, Figure SI3). The decrease of normalized peak heights of L gels is shown in Figure 5. The decrease of peak height with time was fitted to an exponential equation with a retention time τ and a constant baseline c (eq 3),

$$\frac{H(t)}{H(0)} = a \exp\left(\frac{-t}{\tau}\right) + c \quad (3)$$

and the results are listed in Table 2. Figure 5a shows the decrease in the peak height of sample AL1 at temperatures ranging from 25 to 35 °C. As expected, the rate of dehydration increased with the increase of temperatures, as reflected in the decrease of the retention times (Table 2). In addition,

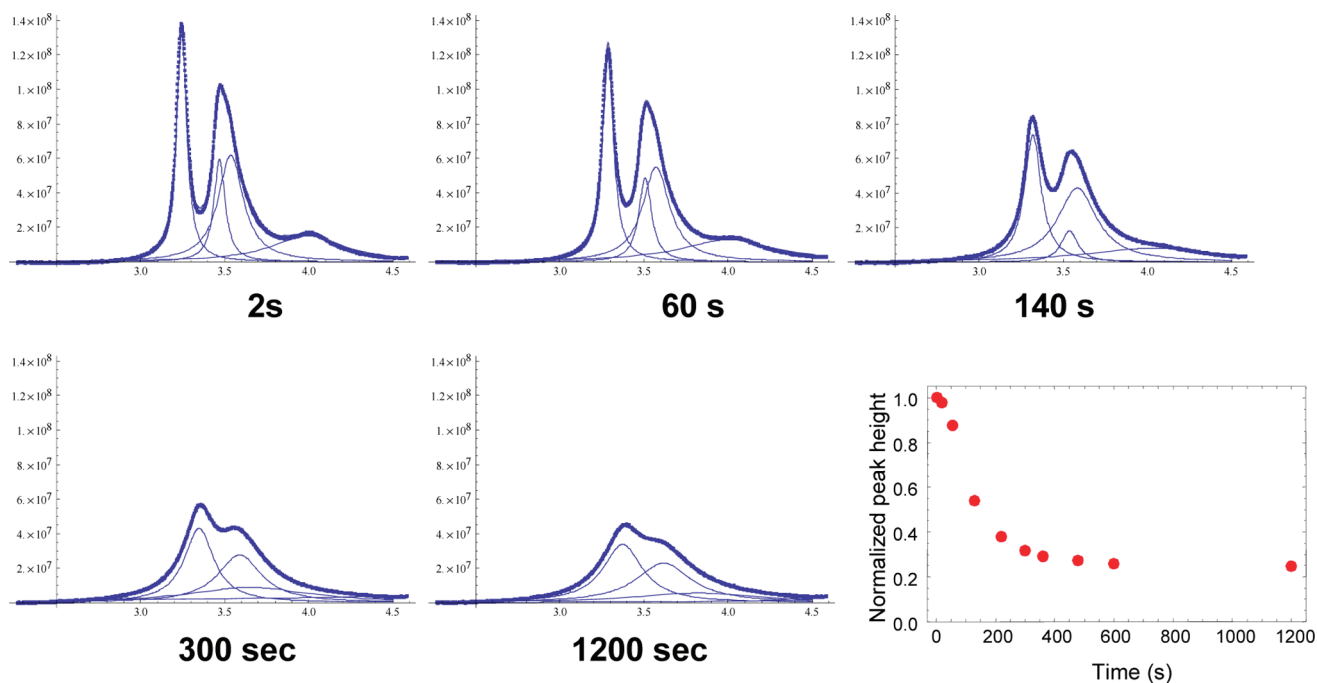


Figure 4. Deconvoluted NMR spectra of low-cross-link density ATRP gel AL1 at 25 °C at selected times. Upfield and downfield are inverted for a calculation purpose.

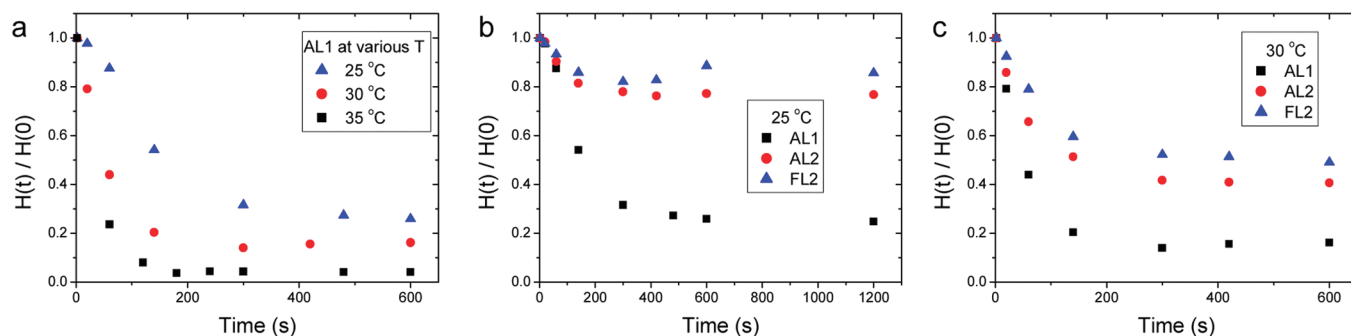


Figure 5. Decrease of peak height of variable-temperature time-lapse ^1H NMR spectra of low-cross-link density gels (L gels). (a) ATRP gel AL1 at different temperature; (b) L gels at 25 °C; (c) L gels at 30 °C.

Table 2. Retention Times (τ (s)) and Baseline (c) Terms of Hydrogel's Dehydration Kinetics^a

temp (°C)	AH1 ^b		AL1		AL2		FL2	
	τ	c	τ	c	τ	c	τ	c
25			147	0.22				
30	208	0.21	54	0.13	71	0.49	95	0.41
35			37	0.08				

^a Based on the evolutions of methoxy peak (~ 3.2 ppm) heights in ^1H NMR spectra. ^b For high-cross-link density gels (H gels), only one data set was available due to the experimental difficulty.

the overall level of dehydration after 10 min increased with the increase of temperature, as manifested by the lowering of the constant baseline (Figure 5a and Table 2). At a given temperature, the magnitude of dehydration retention time (τ) was inversely proportional to the swelling ratio, which was, in turn, proportional to the degree of cross-linking. This was because hydrogen bonding in a more densely cross-linked hydrogel is more resistant to disruption.⁶⁸ Comparing the ATRP and FRP gels, the dehydration of AL2 was faster than FL2, although the gel conversion values were quite comparable. The ATRP gel AL2 has a lower net cross-linking density due to the minimized amount of dense

nanogel domains, where $H(t)$ is the peak height at time t , $H(0)$ is the initial peak height, and $a + c = 1$.

4. Comparison of Macroscopic Deswelling and Molecular Level Dehydration Kinetics. The kinetics of macroscopic deswelling and molecular level dehydration results of the low-cross-link density gels (L gels) are compared in Figure 6. The dehydration of polymer chains assessed by ^1H NMR reached a plateau after 300 s, while the actual deswelling progressed for a longer time period. For example, the ^1H NMR peak height for AL2 appeared to saturate at the 40% level in ca. 300 s (Figure 6b). However, as inferred from macroscopic volumetric analysis, only 30% of absorbed water had been released and deswelling progressed on a time scale which was at least 1 order of magnitude longer (Figure 6a). The apparent discrepancy can be easily understood once one realizes that collapse (dehydration) of polymer chains does not imply immediate removal of water from the partially collapsed network. Following the chain collapse, water still needs to travel to the surface of the sample through the network of "diffusion channels". Moreover, as discussed earlier, the final water release from the gel may be significantly hindered through the formation of dense collapsed skin at the surface of the sample. At a higher temperature

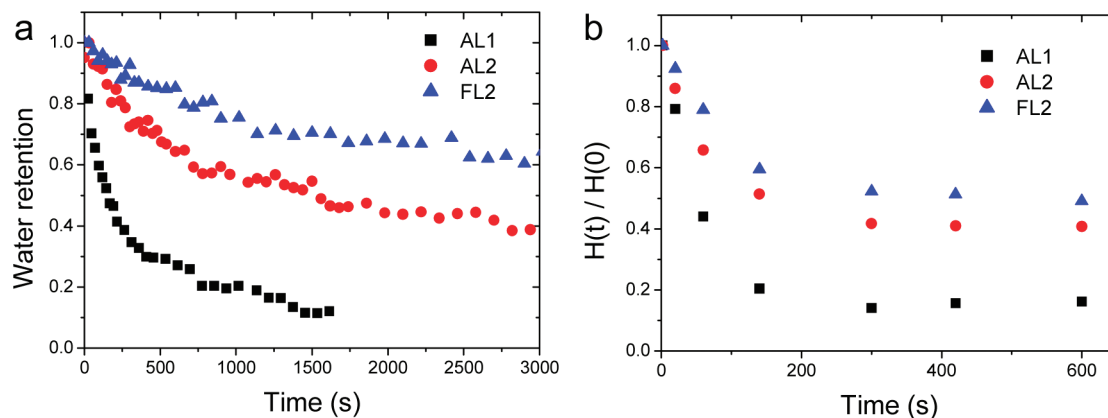


Figure 6. Comparison of macroscopic deswelling of low-cross-link density gels (L gels) (a) to molecular level dehydration (b) at 30 °C.

such as 45 °C, the peak height evolution of ^1H NMR should reach a saturated state in a shorter time, less than 300 s, and the polymer chains should be dehydrated to a higher degree. Nevertheless, the water retention only reached values around 0.5, 0.8, and 0.9 with AL1, AL2, and FL2 at 300 s, respectively, and these numbers even higher than those at 30 °C (0.3, 0.7, and 0.85). Hence, at 45 °C, the water molecules are predominantly retained inside the gel as a consequence of the presence of a hydrophobic shell (skin layer) even though most water molecules lost the interactions to the polymer chains.

Conclusions

Thermoresponsive hydrogels based on MEO₂MA were prepared both by ATRP and FRP. The gels prepared by ATRP displayed higher swelling ratio than FRP gels due to a lower amount of densely cross-linked nanogel domains. When the deswelling rates of high-cross-link density gels (H gels) were compared at temperatures above 45 °C, the ATRP gels deswelled at a slower rate than the FRP gels. More interestingly, the overall deswelling rate was quicker at 30 °C than at 45 °C and slowest at 60 °C for ATRP gels, even though one might expect a faster transition at a higher temperature. This observation could be explained by the more rapid formation of the less permeable skin layer at the higher temperature. The greater susceptibility of ATRP gels to the skin effect was attributed to the more homogeneous network structure, resulting in a uniformly collapsed skin layer and a lack of water diffusion channels. The FRP gels were less affected by such a process, most likely as a result of the structural heterogeneity; the presence of the irregular loosely and densely cross-linked domains in the FRP gels facilitated their faster draining.

For low-cross-link density gels (L gels), the more systematic study was conducted by comparing the macroscopic deswelling with dehydration at the molecular level studied by the variable-temperature time-lapse NMR spectroscopy. The dehydration of polymer chains at the molecular level was always much faster than the macroscopic deswelling. The dehydration rate at molecular level increased with temperature, in contrast to the rate of macroscopic deswelling. Thus, at higher temperatures, skin layer formation significantly reduced the macroscopic deswelling rate in spite of faster dehydration of the polymer chains.

The presented results indicate that macroscopic swelling/deswelling kinetics of CRP hydrogels is controlled not only by network homogeneity but also by the skin effects. One of the possible strategies to overcome the latter limitation could involve controlled introduction of structural/chemical heterogeneity to facilitate the formation of water diffusion channels.

Acknowledgment. The authors are grateful for the financial support provided by the members of the CRP Consortium at

Carnegie Mellon University and NSF (DMR-09-69301). The NMR instrumentation at Carnegie Mellon University was partially supported by NSF (CHE-013093). Also, we acknowledge many helpful discussions with Dr. James Spanswick for this paper.

Supporting Information Available: Experimental details about gel purification and the image analysis method, comparison of results of the gravimetry and image analysis, and more NMR data. This material is available free of charge via the Internet at <http://pubs.acs.org>.

References and Notes

- (1) Alarcon, C. D. H.; Pennadam, S.; Alexander, C. *Chem. Soc. Rev.* **2005**, *34*, 276–285.
- (2) Roy, D.; Cambre, J. N.; Sumerlin, B. S. *Prog. Polym. Sci.* **2010**, *35*, 278–301.
- (3) Liu, F.; Urban, M. W. *Prog. Polym. Sci.* **2010**, *35*, 3–23.
- (4) Aoshima, S.; Kanaoka, S. *Adv. Polym. Sci.* **2008**, *210*, 169–208.
- (5) Soppimath, K. S.; Aminabhavi, T. M.; Dave, A. M.; Kumbar, S. G.; Rudzinski, W. E. *Drug Dev. Ind. Pharm.* **2002**, *28*, 957–974.
- (6) Gupta, P.; Vermani, K.; Garg, S. *Drug Discovery Today* **2002**, *7*, 569–579.
- (7) Qiu, Y.; Park, K. *Adv. Drug Delivery Rev.* **2001**, *53*, 321–339.
- (8) Ehrick, J. D.; Deo, S. K.; Browning, T. W.; Bachas, L. G.; Madou, M. J.; Daunert, S. *Nat. Mater.* **2005**, *4*, 298–302.
- (9) Schepelina, O.; Zharov, I. *Langmuir* **2007**, *23*, 12704–12709.
- (10) Castellanos, A.; DuPont, S. J.; Heim, A. J.; Matthews, G.; Stroot, P. G.; Moreno, W.; Toomey, R. G. *Langmuir* **2007**, *23*, 6391–6395.
- (11) Huck, W. T. S. *Mater. Today* **2008**, *11*, 24–32.
- (12) Wang, J.; Chen, Z. Y.; Mauk, M.; Hong, K. S.; Li, M. Y.; Yang, S.; Bau, H. H. *Biomed. Microdevices* **2005**, *7*, 313–322.
- (13) Yeghiazarian, L.; Mahajan, S.; Montemagno, C.; Cohen, C.; Wiesner, U. *Adv. Mater.* **2005**, *17*, 1869–1873.
- (14) Kim, D.; Beebe, D. J. *Lab Chip* **2007**, *7*, 193–198.
- (15) Kim, J. H.; Lee, T. R. *Langmuir* **2007**, *23*, 6504–6509.
- (16) Jiang, X. W.; Xiong, D. A.; An, Y. L.; Zheng, P. W.; Zhang, W. Q.; Shi, L. Q. *J. Polym. Sci., Part A: Polym. Chem.* **2007**, *45*, 2812–2819.
- (17) Schexnailder, P.; Schmidt, G. *Colloid Polym. Sci.* **2009**, *287*, 1–11.
- (18) Schild, H. G. *Prog. Polym. Sci.* **1992**, *17*, 163–249.
- (19) Kaneko, Y.; Nakamura, S.; Sakai, K.; Aoyagi, T.; Kikuchi, A.; Sakurai, Y.; Okano, T. *Macromolecules* **1998**, *31*, 6099–6105.
- (20) Wang, X. H.; Qiu, X. P.; Wu, C. *Macromolecules* **1998**, *31*, 2972–2976.
- (21) Lutz, J. F.; Akdemir, O.; Hoth, A. *J. Am. Chem. Soc.* **2006**, *128*, 13046–13047.
- (22) Lutz, J. F.; Andrieu, J.; Uzun, S.; Rudolph, C.; Agarwal, S. *Macromolecules* **2007**, *40*, 8540–8543.
- (23) Lutz, J. F.; Weichenhan, K.; Akdemir, O.; Hoth, A. *Macromolecules* **2007**, *40*, 2503–2508.
- (24) Yamamoto, S.; Pietrasik, J.; Matyjaszewski, K. *Macromolecules* **2007**, *40*, 9348–9353.
- (25) Yamamoto, S. I.; Pietrasik, J.; Matyjaszewski, K. *J. Polym. Sci., Part A: Polym. Chem.* **2008**, *46*, 194–202.

- (26) Cai, T.; Marquez, M.; Hu, Z. B. *Langmuir* **2007**, *23*, 8663–8666.
- (27) Matyjaszewski, K.; Davis, T. P. *Handbook of Radical Polymerization*; Wiley-Interscience: Hoboken, 2002.
- (28) Braunecker, W. A.; Matyjaszewski, K. *Prog. Polym. Sci.* **2007**, *32*, 93–146.
- (29) Matyjaszewski, K.; Gnanou, Y.; Leibler, L. *Macromolecular Engineering: From Precise Macromolecular Synthesis to macroscopic Materials Properties and Applications*; Wiley-VCH: Weinheim, 2007.
- (30) Matyjaszewski, K.; Beers, K. L.; Kern, A.; Gaynor, S. G. *J. Polym. Sci., Part A: Polym. Chem.* **1998**, *36*, 823–830.
- (31) Hutchison, J. B.; Stark, P. F.; Hawker, C. J.; Anseth, K. S. *Chem. Mater.* **2005**, *17*, 4789–4797.
- (32) Jin, S. P.; Liu, M. Z.; Chen, S. L.; Gao, C. M. *Eur. Polym. J.* **2008**, *44*, 2162–2170.
- (33) Taton, D.; Baussard, J. F.; Dupayage, L.; Poly, J.; Gnanou, Y.; Ponsinet, V.; Destarac, M.; Mignaud, C.; Pitois, C. *Chem. Commun.* **2006**, 1953–1955.
- (34) Liu, Q. F.; Zhang, P.; Qing, A. X.; Lan, Y. X.; Lu, M. G. *Polymer* **2006**, *47*, 2330–2336.
- (35) Tai, H. Y.; Howard, D.; Takae, S.; Wang, W. X.; Vermonden, T.; Hennink, W. E.; Stayton, P. S.; Hoffman, A. S.; Endruweit, A.; Alexander, C.; Howdle, S. M.; Shakesheff, K. M. *Biomacromolecules* **2009**, *10*, 2895–2903.
- (36) Xu, F. J.; Kang, E. T.; Neoh, K. G. *Biomaterials* **2006**, *27*, 2787–2797.
- (37) Fechler, N.; Badi, N.; Schade, K.; Pfeifer, S.; Lutz, J. F. *Macromolecules* **2009**, *42*, 33–36.
- (38) Bencherif, S. A.; Siegwart, D. J.; Srinivasan, A.; Horkay, F.; Hollinger, J. O.; Washburn, N. R.; Matyjaszewski, K. *Biomaterials* **2009**, *30*, 5270–5278.
- (39) Li, C. M.; Madsen, J.; Armes, S. P.; Lewis, A. L. *Angew. Chem., Int. Ed.* **2006**, *45*, 3510–3513.
- (40) Yu, Q.; Xu, S. H.; Zhang, H. W.; Ding, Y. H.; Zhu, S. P. *Polymer* **2009**, *50*, 3488–3494.
- (41) Mespouille, L.; Coulembier, O.; Paneva, D.; Degee, P.; Rashkov, I.; Dubois, P. *Chem.—Eur. J.* **2008**, *14*, 6369–6378.
- (42) Ide, N.; Fukuda, T. *Macromolecules* **1999**, *32*, 95–99.
- (43) Gao, H. F.; Matyjaszewski, K. *Prog. Polym. Sci.* **2009**, *34*, 317–350.
- (44) Tsarevsky, N. V.; Matyjaszewski, K. *Macromolecules* **2005**, *38*, 3087–3092.
- (45) Taton, D.; Baussard, J. F.; Dupayage, L.; Poly, J.; Gnanou, Y.; Ponsinet, V.; Destarac, M.; Mignaud, C.; Pitois, C. *Chem. Commun.* **2006**, 18, 1953–1955.
- (46) Oh, J. K.; Tang, C.; Gao, H.; Tsarevsky, N. V.; Matyjaszewski, K. *J. Am. Chem. Soc.* **2006**, *128*, 5578–5584.
- (47) Oh, J. K.; Siegwart, D. J.; Lee, H.-i.; Sherwood, G.; Peteanu, L.; Hollinger, J. O.; Kataoka, K.; Matyjaszewski, K. *J. Am. Chem. Soc.* **2007**, *129*, 5939–5945.
- (48) Oh, J. K.; Lee, D. I.; Park, J. M. *Prog. Polym. Sci.* **2009**, *34*, 1261–1282.
- (49) Oh, J. K.; Drumright, R.; Siegwart, D. J.; Matyjaszewski, K. *Prog. Polym. Sci.* **2008**, *33*, 448–477.
- (50) Bencherif, S. A.; Washburn, N. R.; Matyjaszewski, K. *Biomacromolecules* **2009**, *10*, 2499–2507.
- (51) Atzet, S.; Curtin, S.; Trinh, P.; Bryant, S.; Ratner, B. *Biomacromolecules* **2008**, *9*, 3370–3377.
- (52) Oh, J. K.; Bencherif, S. A.; Matyjaszewski, K. *Polymer* **2009**, *50*, 4407–4423.
- (53) Wang, J. S.; Matyjaszewski, K. *J. Am. Chem. Soc.* **1995**, *117*, 5614–5615.
- (54) Patten, T. E.; Xia, J. H.; Abernathy, T.; Matyjaszewski, K. *Science* **1996**, *272*, 866–868.
- (55) Tsarevsky, N. V.; Matyjaszewski, K. *Chem. Rev.* **2007**, *107*, 2270–2299.
- (56) Matyjaszewski, K.; Tsarevsky, N. V. *Nat. Chem.* **2009**, *1*, 276–288.
- (57) Matyjaszewski, K.; Xia, J. H. *Chem. Rev.* **2001**, *101*, 2921–2990.
- (58) Zhang, X. Z.; Wang, F. J.; Chu, C. C. *J. Mater. Sci., Mater. Med.* **2003**, *14*, 451–455.
- (59) Kaneko, Y.; Sakai, K.; Kikuchi, A.; Yoshida, R.; Sakurai, Y.; Okano, T. *Macromolecules* **1995**, *28*, 7717–7723.
- (60) Gao, H.; Min, K.; Matyjaszewski, K. *Macromolecules* **2007**, *40*, 7763–7770.
- (61) Gao, H. F.; Li, W. W.; Matyjaszewski, K. *Macromolecules* **2008**, *41*, 2335–2340.
- (62) The hydroxyl group of HEMA is converted to a 2-bromoiso-butyrate group that can initiate a “graft-from” ATRP and to grow a dangling chain from each initiation site.
- (63) Fernandez, V. V. A.; Tepale, N.; Sanchez-Diaz, J. C.; Mendizabal, E.; Puig, J. E.; Soltero, J. F. A. *Colloid Polym. Sci.* **2006**, *284*, 387–395.
- (64) Nayak, S.; Debord, S. B.; Lyon, L. A. *Langmuir* **2003**, *19*, 7374–7379.
- (65) Kim, J. H.; Lee, S. B.; Kim, S. J.; Lee, Y. M. *Polymer* **2002**, *43*, 7549–7558.
- (66) Morimoto, N.; Ohki, T.; Kurita, K.; Akiyoshi, K. *Macromol. Rapid Commun.* **2008**, *29*, 672–676.
- (67) Van Durme, K.; Van Mele, B.; Loos, W.; Du Prez, F. E. *Polymer* **2005**, *46*, 9851–9862.
- (68) Dai, H. J.; Chen, Q.; Qin, H. L.; Guan, Y.; Shen, D. Y.; Hua, Y. Q.; Tang, Y. L.; Xu, J. *Macromolecules* **2006**, *39*, 6584–6589.